

The evolution of mapping habitat for northern spotted owls (*Strix occidentalis caurina*): A comparison of photo-interpreted, Landsat-based, and lidar-based habitat maps

The Faculty of Oregon State University has made this article openly available.
Please share how this access benefits you. Your story matters.

Citation	Ackers, S. H., Davis, R. J., Olsen, K. A., & Dugger, K. M. (2015). The evolution of mapping habitat for northern spotted owls (<i>Strix occidentalis caurina</i>): A comparison of photo-interpreted, Landsat-based, and lidar-based habitat maps. <i>Remote Sensing of Environment</i> , 156, 361-373. doi:10.1016/j.rse.2014.09.025
DOI	10.1016/j.rse.2014.09.025
Publisher	Elsevier
Version	Version of Record
Terms of Use	http://cdss.library.oregonstate.edu/sa-termsfuse



The evolution of mapping habitat for northern spotted owls (*Strix occidentalis caurina*): A comparison of photo-interpreted, Landsat-based, and lidar-based habitat maps



Steven H. Ackers^{a,*}, Raymond J. Davis^b, Keith A. Olsen^c, Katie M. Dugger^d

^a Oregon Cooperative Fish and Wildlife Research Unit, Department of Fisheries and Wildlife, Oregon State University, Corvallis, OR 97331, USA

^b USDA Forest Service, Forestry Sciences Laboratory, 3200 SW Jefferson Way, Corvallis, OR 97331, USA

^c Department of Forest Ecosystems and Society, Oregon State University, Corvallis, OR 97331, USA

^d U.S. Geological Survey, Oregon Cooperative Fish and Wildlife Research Unit, Department of Fisheries and Wildlife, Oregon State University, Corvallis, OR 97331, USA

ARTICLE INFO

Article history:

Received 24 July 2013

Received in revised form 16 September 2014

Accepted 20 September 2014

Available online 30 October 2014

Keywords:

Landsat TM

Lidar

Northern spotted owl

Habitat suitability

Maxent

Species distribution modeling

GNN

ABSTRACT

Wildlife habitat mapping has evolved at a rapid pace over the last few decades. Beginning with simple, often subjective, hand-drawn maps, habitat mapping now involves complex species distribution models (SDMs) using mapped predictor variables derived from remotely sensed data. For species that inhabit large geographic areas, remote sensing technology is often essential for producing range wide maps. Habitat monitoring for northern spotted owls (*Strix occidentalis caurina*), whose geographic covers about 23 million ha, is based on SDMs that use Landsat Thematic Mapper imagery to create forest vegetation data layers using gradient nearest neighbor (GNN) methods. Vegetation data layers derived from GNN are modeled relationships between forest inventory plot data, climate and topographic data, and the spectral signatures acquired by the satellite. When used as predictor variables for SDMs, there is some transference of the GNN modeling error to the final habitat map. Recent increases in the use of light detection and ranging (lidar) data, coupled with the need to produce spatially accurate and detailed forest vegetation maps have spurred interest in its use for SDMs and habitat mapping. Instead of modeling predictor variables from remotely sensed spectral data, lidar provides direct measurements of vegetation height for use in SDMs. We expect a SDM habitat map produced from directly measured predictor variables to be more accurate than one produced from modeled predictors.

We used maximum entropy (Maxent) SDM modeling software to compare predictive performance and estimates of habitat area between Landsat-based and lidar-based northern spotted owl SDMs and habitat maps. We explored the differences and similarities between these maps, and to a pre-existing aerial photo-interpreted habitat map produced by local wildlife biologists. The lidar-based map had the highest predictive performance based on 10 bootstrapped replicate models ($AUC = 0.809 \pm 0.011$), but the performance of the Landsat-based map was within acceptable limits ($AUC = 0.717 \pm 0.021$). As is common with photo-interpreted maps, there was no accuracy assessment available for comparison. The photo-interpreted map produced the highest and lowest estimates of habitat area, depending on which habitat classes were included (nesting, roosting, and foraging habitat = 9962 ha, nesting habitat only = 6036 ha). The Landsat-based map produced an estimate of habitat area that was within this range (95% CI: 6679–9592 ha), while the lidar-based map produced an area estimate similar to what was interpreted by local wildlife biologists as nesting (i.e., high quality) habitat using aerial imagery (95% CI: 5453–7216). Confidence intervals of habitat area estimates from the SDMs based on Landsat and lidar overlapped.

We concluded that both Landsat- and lidar-based SDMs produced reasonable maps and area estimates for northern spotted owl habitat within the study area. The lidar-based map was more precise and spatially similar to what local wildlife biologists considered spotted owl nesting habitat. The Landsat-based map provided a less precise spatial representation of habitat within the relatively small geographic confines of the study area, but habitat area estimates were similar to both the photo-interpreted and lidar-based maps.

Photo-interpreted maps are time consuming to produce, subjective in nature, and difficult to replicate. SDMs provide a framework for efficiently producing habitat maps that can be replicated as habitat conditions change over time, provided that comparable remotely sensed data are available. When the SDM uses predictor variables extracted from lidar data, it can produce a habitat map that is both accurate and useful at large and small spatial

* Corresponding author at: H.J. Andrews Experimental Forest, P.O. Box 300, Blue River, Oregon, USA. Tel.: +1 541 822 3359; fax: +1 541 822 6329.
E-mail address: ackerss@onid.orst.edu (S.H. Ackers).

scales. In comparison, SDMs using Landsat-based data are more appropriate for large scale analyses of amounts and general spatial patterns of habitat at regional scales.

© 2014 Elsevier Inc. All rights reserved.

1. Introduction

Less than two years after the 1972 launch of the first Landsat Thematic Mapper satellite (Earth Resources Technology Satellite 1), the color infrared imagery collected by its multispectral scanner was interpreted and used to make a map of northern spotted owl (*Strix occidentalis caurina*) habitat. That map showed that a proposed timber sale in the Coast Range of Oregon would impact the owl's nesting habitat and it was subsequently halted (Mouat & Schruppf, 1974). Since then, and largely due to the loss of its habitat, the northern spotted owl was listed as threatened under the U.S. Endangered Species Act (USDI, 1990). Consequently, northern spotted owl habitat maps have played an ever increasing role in land management and conservation for this subspecies.

The northern spotted owl is associated with older coniferous forests of the Pacific Northwest region of the United States (e.g., Carey, Reid, & Horton, 1990; Forsman, Meslow, & Wight, 1984; Ripple, Lattin, Hershey, Wagner, & Meslow, 1997). In the Cascade Mountains of Oregon, they typically inhabit forest stands dominated by Douglas-fir (*Pseudotsuga menziesii*) and western hemlock (*Tsuga heterophylla*) and which include multiple age classes of trees forming a multi-layered canopy (Forsman et al., 1984). These older forests usually show a high degree of decadence (e.g., damaged or dead trees and downed wood) that provides structures associated with spotted owl nesting, roosting, and foraging habitat (Hershey, Meslow, & Ramsey, 1998; North, Franklin, Carey, Forsman, & Hamer, 1999). Several studies have provided a wealth of information about structural parameters of spotted owl habitat such as average tree diameter, density of large trees, basal area, canopy cover, vertical canopy structure, and the diversity of tree size classes (e.g., Carey et al., 1990; Hershey et al., 1998; McComb, McGrath, Spies, & Vesely, 2002; North et al., 1999; Ripple et al., 1997; Solis & Gutierrez, 1990; Swindle, Ripple, Meslow, & Schafer, 1999). These characteristics produce forest canopy heterogeneity that is visible in aerial photographs (Cohen, Spies, & Bradshaw, 1990) and can be identified by particular spectral characteristics from satellite imagery of the forests within the northern spotted owl's range (Cohen, Maieringer, Spies, & Oetter, 2001; Cohen & Spies, 1992).

The first northern spotted owl habitat maps were hand drawn interpretations of remotely sensed data that were passively collected from either airborne or spaceborne platforms. The interpretation of that imagery into habitat classes was subject to the mapper's experience and understanding of the how the owl uses the forest, based on the research of the time. Habitat classes were delineated as polygons that corresponded to differences in tree species composition and stand structure visible in the imagery. Most of these maps covered small landscapes (<12,000 ha) and contained one to several owl territories (Forsman et al., 1984). While these maps were useful for project planning and land management at a local scale, it was usually infeasible to produce them at a watershed or regional scale.

Our ability to map spotted owl habitat improved with the advent of species distribution modeling software, advances in geographic information systems, and remote sensing technologies. These advances allowed us to produce range-wide habitat maps for this subspecies, covering over 23 million ha (Davis, Dugger, Mohoric, Evers, & Aney, 2011; Lint, 2005). More importantly, we could then monitor habitat change and trends through time using time-series Landsat Thematic Mapper (TM) imagery (Davis et al., 2011).

Maps of forest vegetation derived from Landsat TM imagery combined with regional environmental variables served as the environmental predictor variables used to model and map spotted owl habitat (Davis et al., 2011; Lint, 2005). These Landsat-derived variables were

themselves inferred from modeled relationships between spectral signals and ground conditions (e.g., Ohmann & Gregory, 2002; Ohmann et al., 2012). Some of the error inherent in the modeling process was transferred to the habitat maps. Forest structure data layers derived from lidar are based on measurements of forest vegetation height and density at a much finer spatial resolution (Bergen et al., 2009; Lefsky, Cohen, Parker, & Harding, 2002). This high resolution data allows direct measurements and estimates of the within-stand variation of the structural characteristics of forest stands that are important to spotted owls (Garcia-Feced, Tempel, & Kelly, 2011). We expected that predictive performance of species distribution models (SDMs) based on direct measurements of forest structural parameters would be better than for SDMs based on inferred measurements.

Here, we examined the differences and similarities between two spatially-explicit SDMs for northern spotted owls covering the same geographic area. Our objectives were to (1) compare an SDM using the Landsat data source previously used for the regional northern spotted owl monitoring program (Davis et al., 2011) to an SDM using analogous data extracted from recent lidar acquisitions, (2) compare the relative importance of predictor variables to habitat suitability indices calculated from both data sources, and (3) compare area estimates and spatial patterns of suitable habitat area derived from both data sources and from a pre-existing photo-interpreted habitat map produced by local wildlife biologists.

2. Methods

2.1. Study area

The study area was located in the Blue River watershed on the McKenzie River Ranger District of the Willamette National Forest on the western slope of the Cascade Mountains in Oregon, USA (Fig. 1). It covered 19,000 ha with elevations ranging from 400 m to 1600 m. Douglas-fir and western hemlock were the predominant tree species with stands of Pacific silver fir (*Abies amabilis*) and mountain hemlock (*Tsuga mertensiana*) at higher elevations (Cissel, Swanson, & Weisberg, 1999). The southeast portion of the study area included the H.J. Andrews Experimental Forest, part of the Central Cascades Adaptive Management Area delineated under the Northwest Forest Plan (USDA & USDI, 1994). Approximately 5% of the study area was nonforest vegetation, 25% consisted of stands that were clear-cut harvested and replanted between 1950 and 1994, 9% were naturally regenerated young stands between 40 and 80 years old, 25% were mature stands between 80 and 200 years of age, and 36% were old growth stands greater than 200 years old (Cissel et al., 1999). The average size of the stands in the Blue River watershed as delineated in the Willamette National Forest vegetation GIS layer is 17.4 ha (95% C.I.: 4.2–30.6 ha) (USFS, 2007a).

2.2. Northern spotted owl presence data

We obtained nest and daytime roost locations of territorial northern spotted owl pairs following a standardized protocol as part of a regional spotted owl monitoring project (Forsman, 1999). Initial detections occurred during nighttime surveys while broadcasting recorded spotted owl calls from predetermined survey stations systematically placed 0.5–0.8 km along forest roads and trails throughout the watershed. We determined the location of each nighttime detection by estimating the distance to the vocalizing spotted owl and plotting the azimuth on a topographic map. We obtained more precise locations for use in habitat mapping by returning to these areas the following day and locating roosting owls, again using playbacks of spotted owl calls to elicit

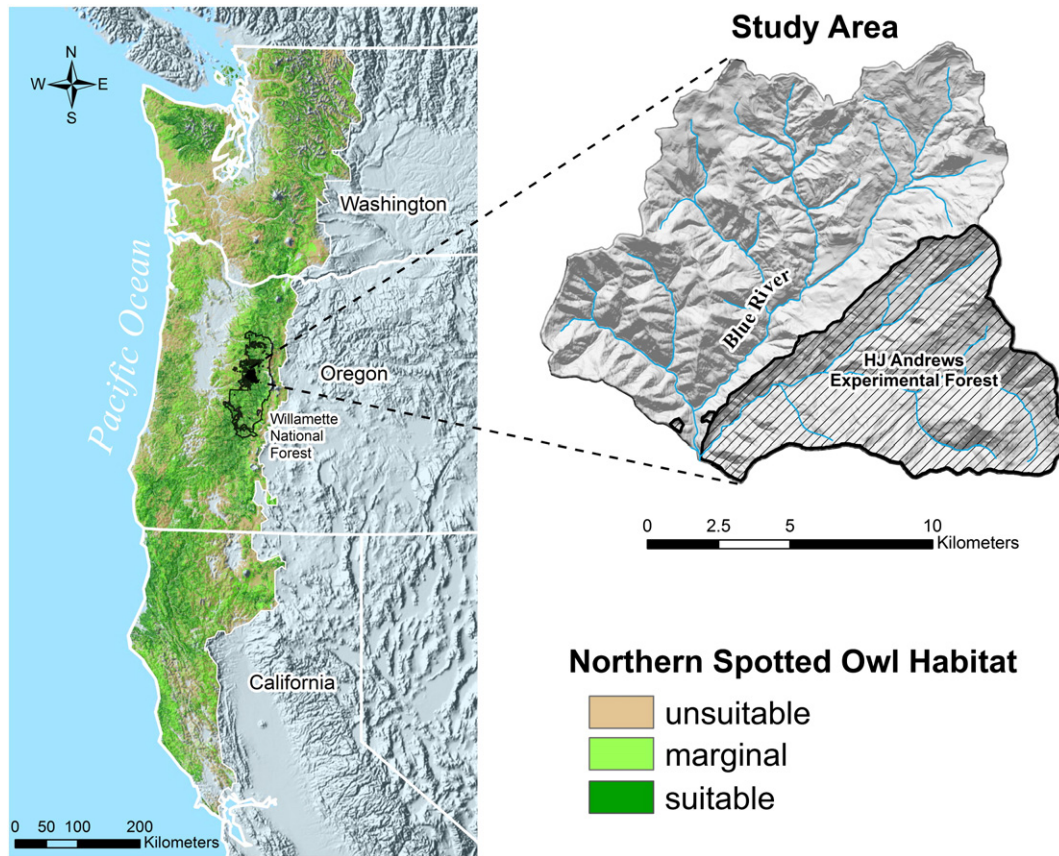


Fig. 1. Range-wide map of northern spotted owl habitat in the Pacific Northwest of the United States and location of the study area on the Willamette National Forest. Habitat classifications are based on gradient nearest neighbor (GNN) models using Landsat TM and environmental predictor variables (Davis et al., 2011; Ohmann & Gregory, 2002).

vocalizations from the owls. We did not use the initial nighttime detections in this analysis. Once a pair of owls was visually located, we determined their nesting status and recorded the location of the nest tree to within 10 m using GPS. Nest trees that were used in multiple years were present in the data set only once. In years that pairs did not nest, we plotted the earliest daytime roost location for each non-nesting pair on topographic maps to represent the best annual location for each pair *in lieu* of a nest. We excluded the locations of unpaired owls because we were focusing on pairs that held stable territories. The final data set contained one location per year for each pair of owls located from 1990 to 1999, and the final data set contained 159 nest and roost locations.

We did not use any northern spotted owl locations from more recent surveys (2000–2014) to avoid potential biases with habitat selection influenced by interspecific competition with barred owls (*Strix varia*), a more aggressive owl that shares many of the same habitat preferences as the spotted owl, and that have become increasingly common since 2000 (e.g., Hamer, Forsman, & Glenn, 2007; Kelly, Forsman, & Anthony, 2003; Wiens, Anthony, & Forsman, 2011). When spotted owls are displaced from their territories by barred owls, we expect the spotted owls to occupy less suitable habitat than they would select in the absence of barred owls (Dugger, Anthony, & Andrews, 2011). Given that there was little change in the amount available habitat in the Blue River watershed between 1999 and 2011 (R. Seitz, personal communication, March 6, 2014), we felt that the accelerated increase in barred owl detections after 2000 would produce a greater bias than differences in the amount of available habitat between the periods 1990–1999 and 2000–2011.

2.3. Landsat-based predictor variables

Ohmann et al. (2012) used 2006 Landsat TM imagery, climate, and topography data imputed to forest inventory plots measured from 2001 to 2008 to create data layers estimating vegetation structure and

composition. Their imputation technique, gradient nearest neighbor imputation (GNN), involved assigning measured values of vegetation structure from forest inventory plot sample data to each unsampled pixel in their data layers based on the relationships between the plot values and the spectral and environmental data describing the biophysical environment (Eskelson, Temesgen, & Barrett, 2009; Ohmann & Gregory, 2002). Species composition was inferred similarly based on the relationships between the relative basal areas of particular tree species and the spectral and environmental data (Ohmann & Gregory, 2002). All predictor variable layers were scaled to a 30 m grid size to maintain consistency between the mapped distribution of forest characteristics and field plots when the GNN variable rasters were created (Ohmann et al., 2012). Davis et al. (2011) used these inferred data layers of vegetation structure and composition as predictor variables in SDMs of northern spotted owl habitat. Here, we refer to these data layers simply as the Landsat-based predictor variables.

Of the initial set of 11 predictor variables derived by Davis et al. (2011), we selected five forest structure variables, and one species composition variable that estimated the percentage of total basal area of high elevation forest conifer species such as true firs (*Abies* spp.) and mountain hemlock (*T. mertensiana*). We examined the Pearson's correlation coefficients between potential predictor variable data layers using the Band Collection Statistics tool in ArcMap (ESRI, 2009). We considered pairwise map correlation coefficients, the correlation between plot measurements and imputed values (only available for the Landsat predictor variables, see Davis et al., 2011), and relevance to spotted owl ecology in making our final predictor map selections. Pairwise correlation coefficients greater than 0.70 generally were considered too highly correlated for both predictor variables to be included in the models. When two Landsat predictor variables were highly correlated, we retained the variable with the highest correlation between plot measurements and imputed values (Davis et al., 2011). We made

one exception to the predictor variable correlation rule for the average stand height and the diameter diversity index variables derived from Landsat ($r = 0.73$). In this case, the diameter diversity index had higher plot accuracy, but average stand height was the most comparable to the lidar measurement of tree heights (see Section 2.4). Given that one of our objectives was to compare models based on Landsat versus lidar data sources, we decided to keep both predictor variables to insure that the models from both sources were comparable. We also discarded stand age and kept the density of large conifers, again to be more comparable to the measurements obtained from the lidar data. Our final Landsat model set consisted of four structural variables and one species composition variable (Table 1).

2.4. Lidar-based predictor variables

We used discrete-return airborne lidar data acquired from the H.J. Andrews Experimental Forest in August, 2008 and the remainder of the Blue River watershed in October, 2011 by Watershed Sciences, Inc. (Corvallis, Oregon, USA). They used a Leica ALS60 Phase II sensor mounted in a Cessna Caravan 208B flown at 900 m above ground level. The sensor scan angle was $\pm 14^\circ$ with a scan swath overlap of $\geq 50\%$. Laser pulse rate was 105 kHz and pulse density was ≥ 9 pulses/m² with up to 4 returns per pulse. Accuracy was determined using 344 and 419 ground-based real-time kinematic GPS measurements as reference points for the H.J. Andrews and Blue River watershed data, respectively. Absolute vertical accuracy was 2.4 cm RMSE (H.J. Andrews) and 5.2 cm RMSE (Blue River watershed). Canopy height and bare earth elevation data layers were produced at 1 m resolution. Lidar predictor variable data layers were generated at 30 m resolution directly from the point clouds with program FUSION (McGaughey, 2012) to correspond to the Landsat data resolution. We did not examine the lidar predictor variables at 20 m or 10 m scales because we felt that within-stand variability would increase classification uncertainty to the point that predictive performance would be compromised.

Program FUSION (McGaughey, 2012) was used to create seven lidar predictor variables for cover and height analogous to our Landsat forest structure variables. It also was used to create a field validated stem map of large conifers >76 cm diameter at breast height (d.b.h.) based on local height–diameter relationships (Garman, Acker, Ohmann, & Spies, 1995). We used a kernel density mapping tool in ArcMap Spatial Analyst using a 3 pixel (90 m) search radius to convert the stem map into a density map for large conifers, similar to the Landsat large tree density

variable. We used the Rumple Index (Kane et al., 2010; Parker et al., 2004) as our forest structural heterogeneity predictor variable. This was calculated by averaging the canopy height model (CHM, height of first returns) over a 3×3 window to preserve macro heterogeneity and then running it through the FUSION (McGaughey, 2012) gridSurfaceStats command to produce a ratio of the surface area of the CHM to the surface area of the bare earth digital elevation model. Higher values of this ratio indicated a more complex stand structure. We also calculated four vegetative cover variables: total cover (all returns > 2 m), understory cover (returns between 2 m and 16 m), overstory cover (all returns > 16 m), and the ratio of overstory to understory cover. Finally, we also calculated mean tree height, and mean above-ground biomass for each 30 m grid cell.

As with the Landsat predictor variables, we examined the Pearson's correlation coefficients between potential predictor variable data layers using the Band Collection Statistics tool in ArcMap (ESRI, 2009). When two lidar predictor variables were highly correlated, we retained the variable which was most similar to habitat measurements taken during past spotted owl research. We considered using the lidar estimate of mean aboveground biomass, but decided against it because it was highly correlated with tree density and mean tree height, two measures that were taken directly from lidar data and have been shown to be important components of spotted owl habitat in most stand-level studies (e.g., Hershey et al., 1998; North et al., 1999; Solis & Gutierrez, 1990). Overstory cover and the overstory:understory ratio also were highly correlated with mean tree height, and understory cover was highly correlated with overstory cover. We decided on using total cover greater than 2 m above ground to represent total forest cover. Our final selection included four predictor variables from the lidar data. We also included the high elevation forest predictor variable derived by Davis et al. (2011) because it was important in defining the habitat use in the study area, but it was not measurable with lidar (Table 1).

2.5. Photo-interpreted habitat map

The Willamette National Forest produced a forest-wide map of northern spotted owl habitat in 1991 based on photo interpretation of 1:15,480 scale orthorectified aerial photos. The mapping followed instructions sent to each Ranger District on the Forest (USFS, 2007b). Maps from each Ranger District were reviewed by local wildlife biologists and compiled into one forest-wide map. This map is updated annually, using interpretation of the most recent aerial imagery and

Table 1
Definitions of the predictor variables used in the (a) Landsat and (b) lidar based spotted owl habitat suitability models.

	Variable	Description	Units
Landsat model variables (Davis et al., 2011)	Stand height	Average height of dominant and co-dominant trees	Meters
	Forest cover	Percentage of cover in the canopy as calculated using the Forest Vegetation Simulator methodology (Dixon et al., 2002)	Percentage
	Density of large conifers	Estimated tree density for all live conifers ≥ 76 cm d.b.h.	Trees per hectare
	Diameter diversity index	Index of the structural diversity of a forest stand based on tree densities in different d.b.h. classes. Calculation procedures are described in Appendix 1 of McComb et al. (2002)	Index
	High elevation forest	Stand component of Pacific silver fir (<i>Abies amabilis</i>), (<i>Abies lasiocarpa</i>), noble fir (<i>Abies procera</i>), Shasta red fir (<i>Abies shastensis</i>), Alaska cedar (<i>Chamaecyparis nootkatensis</i>), Engelmann spruce (<i>Picea engelmannii</i>), whitebark pine (<i>Pinus albicaulis</i>), and mountain hemlock (<i>Tsuga mertensiana</i>)	Percentage total basal area
Lidar model variables	Stand height	Mean height of first returns calculated at a 30×30 m resolution	Meters
	Forest cover	Proportion of returns > 2 m above ground calculated at a 30×30 m resolution	Percentage
	Density of large conifers	A kernel density estimate using a 90 m radius for the CanopyMaxima stem map of trees ≥ 47 m in height, which based on local height:diameter data equates to ≥ 76 cm. d.b.h.	Trees per hectare
	Rumple index	A measure of the structural diversity of a forest stand based on ratio of the surface area of the canopy height model to the surface area of the bare earth digital elevation model (Kane et al., 2010; Parker et al., 2004).	Index
	High elevation forest	(same as the Landsat model)	Percentage total basal area

on-the-ground knowledge of conditions and owl locations. The map covers only National Forest lands and consists of 4 classes of owl habitat: 1) nesting, 2) roosting and foraging, 3) dispersal, and 4) unsuitable (Table 2). Forest age and structural attributes are easily observed on high resolution aerial photographs and delineated into stand polygons. Patterns of forest species composition are more subtle and easy to misclassify during this process, and are not included in the Willamette National Forest definition of spotted owl habitat. Habitat polygons ranged in size from 0.4 to 1300 ha within the study area, with an average mapping unit of 32 ha. This map provided a means to compare our empirically derived SDM maps with habitat classifications based on field reconnaissance and expert opinion. While we did not consider the photo-interpreted map as a baseline for assessing the accuracy of the SDM maps, we did consider it as a user's representation of habitat to compare to our SDM versions. Our intent was to compare the strengths and weaknesses of each map and to discuss whether the empirical modeling results provide support to the habitat classifications made by local wildlife biologists in producing the photo-interpreted map.

2.6. SDM modeling and habitat mapping

Our SDM approach was similar to that used by Davis et al. (2011), who produced stand scale maps for monitoring changes in northern spotted owl habitat through time. We used maximum entropy modeling (MaxEnt; Phillips, Dudik, & Schapire, 2004; Phillips, Anderson, & Schapire, 2006) to create spatially explicit spotted owl habitat models using stand level forest structure and species composition predictor variables from both Landsat and lidar data trained to the northern spotted owl nest and pair roost data. Non-forested areas (e.g., rocks, meadows, and snow) were masked out from the SDM process.

After selecting the final set of predictor variables, we used 120 (75%) northern spotted owl presence locations randomly selected from the total set of 159 unique locations as training data for 10 bootstrapped replicate models with the regularization parameter set to the default value of 1.0. Each replicate used the 39 (25%) remaining locations to test the model's predictive performance. A random sample of 10,000 background cells was selected for each replicate. We constrained the sample of background cells to the forested portions of the watershed.

We evaluated model fit by varying the regularization multiplier from 0.5 to 2.0 in increments of 0.25 for 7 sets of 10 replicates for each data source. During this procedure we monitored the difference between regularized training gain and test gain to avoid over-fitting the models. Where training gain was higher than test gain, the model was overfit. We also generated predicted versus expected ratio (P/E) curves for each model to evaluate its predictive performance based on the shape of the curves and Spearman rank statistics (Hirzel, Le Lay, Helfer, Randin, & Guisan, 2006). A final evaluation of predictive performance was based on the area under the curve (AUC) statistic (Fielding & Bell,

1997). The best model was the one with similar regularized training and test gain (overlapping 95% confidence intervals), a stable P/E curve producing a high Spearman rank statistic, and the highest test AUC.

We used the logistic output from Maxent as an index of relative suitability of forest structure and species composition for nesting and roosting by territorial northern spotted owl pairs given the values of the environmental predictor variables at a particular raster cell location compared to a random sample of background values within the study area (Elith et al., 2011; Phillips & Dudik, 2008). Pixels with high logistic scores had environmental conditions similar to where territorial northern spotted owls were found nesting or roosting within the study area. This relationship was defined by environmental variable response functions generated by the model. For our final habitat maps, we used the average and standard deviation of the logistic outputs from the bootstrapping procedure to produce maps representing the average and 95% confidence intervals from the SDMs. Following procedures from Hirzel et al. (2006), we reclassified these maps into three habitat classes as follows:

1. Unsuitable — relative logistic probability values that had 95% confidence limits below the $P/E = 1$ threshold. Below this threshold, the model predicted owl locations less than expected by random chance.
2. Marginal — relative logistic probability values that had 95% confidence limits that crossed the $P/E = 1$ threshold. Within these thresholds, the model predicted owl locations no better than random chance.
3. Suitable — relative logistic probability values that had 95% confidence limits above the $P/E = 1$ threshold. Above this threshold the model predicted owl locations better than expected by random chance.

2.7. Map comparison procedure

Our SDM approach was intended to be comparable to that used by Davis et al. (2011) and we used a spatial scale that we believed was appropriate for comparison to the photo-interpreted map. For each habitat model, we created binary maps of suitable spotted owl habitat. The photo-interpreted habitat map was classified into a binary map of “nesting, roosting, and foraging” habitat by combining the “nesting” and “roosting and foraging” classes from the original map. We also classified it into another binary map using only the “nesting” class, because we wanted to determine which photo-interpreted class best matched the suitable habitat class from our models. We generalized the binary maps from the habitat models, which were based on 30 m resolution data, by using a 3×3 majority filtering process to remove pixel noise and make them more comparable to the patch-delineated photo-interpreted map. We produced estimates of habitat area from these binary maps, including 95% confidence intervals from the bootstrapped SDMs. We were not able to produce error bars for the photo-interpreted map, because it was not empirically derived.

We examined patterns of habitat omission and commission between SDM binary (producer's) maps and the photo-interpreted binary (user's) map using both definitions of habitat described above. We also compared the Landsat- and lidar-based maps directly, using the lidar-based map as the user's map.

Finally, we used Map Comparison Kit (v3.2) software (Visser & de Nijs, 2006) to spatially compare similarities in the distribution and spatial pattern of habitat pair wise among the four types of binary maps. This provides Kappa statistics that provide an index of agreement between the map classes in each map, taking into consideration agreement occurring by chance (Cohen, 1960). The overall Kappa is a combination of the map similarity on a cell to cell basis ($Kappa_{loc}$) and the similarity of the distribution of map classes ($Kappa_{histo}$). Kappa values less than 0.2 indicate slight, 0.2–0.4 fair, 0.4–0.6 moderate, 0.6–0.8 substantial, and 0.8–1.0 almost perfect agreement between maps.

Table 2
Aerial photo interpretation instructions used by the Willamette National Forest to map northern spotted owl habitat (USFS, 2007b).

Habitat class	Description
Nesting	Any habitat that has known or suspected nesting activity. Mature forests (70–100+ years) and also multi-storied old growth forests that are ≥ 200 years old, with average d.b.h. ≥ 30 in., and numerous snags and downed logs
Roosting/ foraging	Any habitat that has known or suspected foraging or roosting activity. Stands that have at least 60% canopy cover. Stand structure is not as clearly defined as for nesting habitat. Can be based on proximity to spotted owl activity centers or nesting habitat. Usually stands ≥ 80 years of age, with average d.b.h. ≥ 18 in.
Dispersal	Stands that have at least 40% canopy cover and do not contain structure to support nesting or foraging. Usually stands with average d.b.h. ≥ 11 in.
Unsuitable	Does not meet the above definitions

3. Results

3.1. Landsat-based models

A regularization multiplier of $RM = 1.75$ produced the best model using only the Landsat predictor variables based on the highest AUC value (0.717 ± 0.021) compared to the other RM values and broadly overlapping confidence limits for the regularized training gain (0.377 ± 0.025) and test gain (0.368 ± 0.062). The percent basal area of high elevation forest and average stand height contributed the most to the overall fit (Table 3). Univariate response curves indicated that low levels of the percent basal area of high elevation forest were associated with a higher probability of spotted owl presence (Fig. 2a). The relative probability of spotted owl presence was positively associated with higher values for stand height, forest cover, and tree diameter diversity (Fig. 2a). The probability of spotted owl presence was highest at intermediate large tree densities of approximately 44 large trees/ha. This value was extracted from the univariate response curve and was the point at which the logistic probability began to decrease as large tree density increased (Fig. 2a). The standard deviation of the logistic output value increased quickly at higher densities because of low numbers of grid cells containing greater than 60 large trees/ha (Fig. 2a).

The predicted versus expected ratio curve (Fig. 3a) showed a relative logistic probability threshold of 0.44. The Landsat binary habitat suitability map based on this threshold showed that 8011 ha (95% CI: 6679–9592) in the Blue River watershed is suitable habitat for spotted owls.

3.2. Lidar-based models

The highest AUC value (0.809 ± 0.011) and the least difference between the regularized training gain (0.697 ± 0.037) and test gain (0.680 ± 0.067) were obtained by applying a regularization multiplier of $RM = 1.5$ to the models using the four lidar predictor variables and the high elevation species composition variable imputed from the Landsat data. The percent contribution and permutation importance of this variable indicated that including species composition information improved the regularized training gain by 11%, and AUC estimates decreased by 25.5% when this information was excluded (Table 3).

The density of large trees and average stand height contributed the most to the overall fit (Table 3). Densities of approximately 40 large trees/ha were associated with the highest probability of spotted owl presence (Fig. 2b). As in the Landsat model, the standard deviation of this variable was large at higher densities of large trees. A similar relationship was apparent with the rumple index; the standard deviation

increased quickly as values of the rumple index increased above 55 (Fig. 2b). High values of mean tree height and total forest cover were associated with high probability of spotted owl presence (Fig. 2b). Also as in the Landsat model, the percent basal area of high elevation forest species was negatively associated with the probability of spotted owl presence (Fig. 2b).

The predicted versus expected ratio curve from the best lidar model (Fig. 3b) showed a relative logistic probability threshold of 0.38 for suitable habitat resulting in an estimate of approximately 6359 ha (95% CI: 5453–7216) of suitable spotted owl habitat in the Blue River watershed.

3.3. Map comparisons

The largest estimate of suitable habitat area was from the photo-interpreted map of nesting, roosting, and foraging habitat combined, and the smallest estimate was from the photo-interpreted map of nesting habitat only (Fig. 4). The Landsat model estimated suitable habitat that spanned this range, with the average being about midway between the two photo-interpreted habitat classes and confidence limits nearly equal to each class (Fig. 4). The lidar-based estimate of suitable habitat area was closest to the photo-interpreted binary map of just the “nesting” class, and had overlapping confidence intervals with that estimate (Fig. 4).

The rates of omission relative to the photo-interpreted binary maps were roughly the same for both Landsat- and lidar-based SDM maps (Table 4). Most of the area classified as spotted owl habitat on the photo-interpreted maps omitted by the models was along the higher elevation ridges that surround the watershed (Fig. 5). In the lower elevations, much of the model omission was along stand edges, but also included finer stand-scale heterogeneity such as gaps in the forest canopy that were not captured in the photo-interpreted maps. The omission error was lowest when the SDM maps were compared to each other (Table 4).

The rates of commission between the SDM maps and the photo-interpreted maps were higher for the Landsat-based map than for the lidar-based map (Table 4). The pattern of SDM commission primarily occurred in the lower elevations (Fig. 5). Model commission was two to three times higher for the comparison with the photo-interpreted nesting only map than with the nesting, roosting, and foraging map (Table 4). The commission rate in the lidar-based map was very low compared to the nesting, roosting, and foraging map, but moderate compared to the nesting only map (Table 4). In both SDMs, the largest portion of commission occurred in the northwestern half of the study area, which is covered with younger forests with less developed structure than the older southeastern portion of the study area that has mostly attained forest structure suitable for owl nesting (Fig. 5). The commission of some younger forest as suitable habitat by the Landsat model is comparable to the commission rates between the nesting only map and each SDM map (Table 4).

The results of the spatial similarity analysis indicated that the lidar map had the best overall agreement with the photo-interpreted map (Table 4). The level of agreement between the lidar map and the photo-interpreted map was moderate for habitat classes of “nesting, roosting, and foraging” ($Kappa = 0.494$) and “nesting” only ($Kappa = 0.495$). The Landsat map had fair agreement ($Kappa$ from 0.288 to 0.380) with both photo-interpreted habitat classes (Table 4). In terms of a cell by cell comparison, the lidar map had substantial agreement ($Kappa_{loc} = 0.786$) with the photo-interpreted “nesting, roosting, and foraging” habitat map and moderate agreement ($Kappa_{loc} = 0.517$) with the “nesting” only map. The distribution of mapped habitat classes in the lidar map was most similar to the photo-interpreted “nesting” map ($Kappa_{histo} = 0.957$, Figs. 5 & 6), while the distribution of the Landsat habitat classes was most similar to the “nesting, roosting, and foraging” map ($Kappa_{histo} = 0.800$, Figs. 5 & 7). The Landsat and lidar maps had moderate overall agreement ($Kappa = 0.481$).

Table 3

The relative contributions of each predictor variable averaged over 10 replicate Maxent runs. The percent contribution is the percentage increase in regularized training gain, or model fit, added by including each variable. The permutation importance is calculated by randomly assigning background values to the presence data and expressing the decrease in AUC, or predictive accuracy, as a percentage when a particular variable is randomized.

	Variable	Percent contribution	Permutation importance
Landsat model variables	High elevation forest	36.4	36.7
	Stand height	31.6	30.4
	Density of large conifers	21.9	12.4
	Diameter diversity index	6.2	15.7
	Forest cover	3.8	4.8
Lidar model variables	Density of large conifers	56.5	36.2
	Stand height	25.4	25.7
	High elevation forest ^a	11.4	25.5
	Rumple index	4.6	8.1
	Forest cover	2.1	4.5

^a The Landsat species composition variable “high elevation forest” also was included in the lidar habitat model.

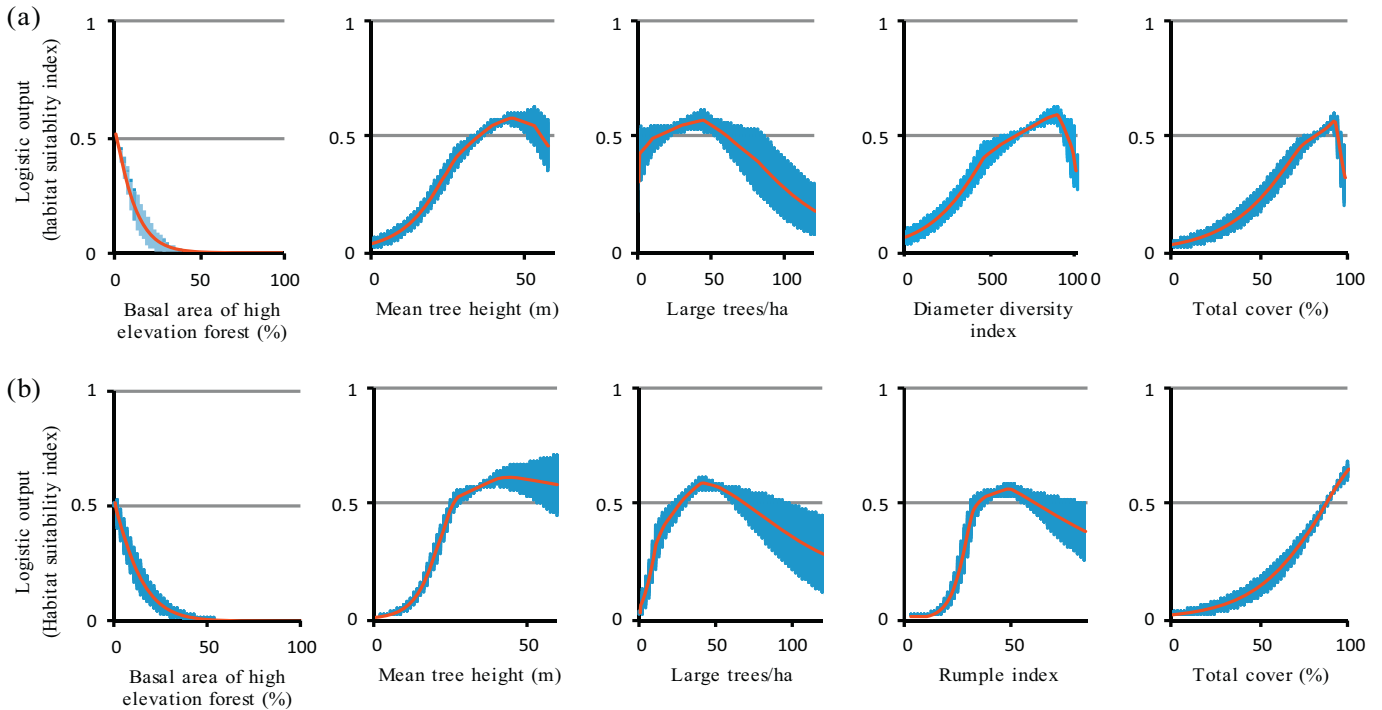


Fig. 2. Univariate response curves for Landsat (a) and lidar (b) based models. The red lines indicate the mean logistic output value, or the habitat suitability index, averaged over 10 replicate runs. The blue shading indicates the standard deviation of the logistic output.

4. Discussion

4.1. Model comparisons

One of our primary objectives was to compare our lidar-based SDM with the Landsat-based SDM used in the northern spotted owl population monitoring program (Davis et al., 2011). We wanted to maintain consistency with that modeling approach so that we would be comparing data sources only and not confound our results with different methodologies. We did not intend to produce a spotted owl habitat model for use by managers because our lidar coverage was limited to just one watershed. A model based on such a limited extent would not be useful except within the confines of that particular watershed.

We assessed the relative importance of each predictor variable by examining their effects on model fit as well as the predictive performance of the model. The percent contribution of each variable (Table 3) reflected the effect of each variable on the regularized training gain, which is an indication of model fit. Permutation importance (Table 3) provided a means of comparing model predictive performance with and without individual variables. The most important predictor variables in the Landsat model of suitable spotted owl habitat were the forest species composition variable that excluded high elevation forest habitat (i.e., the basal area of subalpine tree species) and two indicators of stand age (stand height and density of large conifers; Table 3). These same three variables also explained most of the variation in the lidar model, although they differed in relative importance (Table 3). Based on structural variables alone, the lidar model maintained greater predictive performance than the Landsat model. The direct measurements of the density of large conifers and stand height extracted from lidar contributed 81.9% to model fit, whereas the inferred estimates of these predictors used in the Landsat model together contributed 53.5% to model fit (Table 3).

The basal area of high elevation trees had a strong negative effect on the logistic output estimated by both models by effectively excluding this vegetation type as a component of spotted owl habitat. Excluding the species composition variable from the lidar model decreased the

regularized training gain by 11.4% and decreased the AUC value by 25.5%, while the regularized training gain and AUC for the Landsat model decreased by 36.4% and 36.7%, respectively (Table 3). These results indicated a much greater effect of species composition on the fit of the Landsat model compared to the fit of the lidar model. The importance of species composition variable may have been influenced by the relative strengths of direct measurements as opposed to inferred estimates of the structural variables most closely related to stand age.

Model gain provides a measure of the contrast between the presence locations and the background given the particular combination of variables in a model (Davis et al., 2011). Higher gains indicate a higher contrast between environmental conditions for presence locations compared to the background environmental conditions. Training gain is an index of the level of contrast between the background environmental conditions and the presence locations used to train the model (i.e., model fit), while test gain indicates the level of contrast with the locations used to test the model (i.e., predictive performance). Estimates of the regularized training gain and test gain were roughly equal within each model. This indicated an appropriate level of complexity for both models that resulted in a good balance between model fit and predictive performance. The lidar model produced higher estimates of regularized training gain, which indicated a more precise model fit, and higher estimates of test gain, which indicated higher predictive performance. Overall, the lidar model produced a map with greater contrast between suitable habitat and unsuitable habitat, than the Landsat model.

The mathematical relationships between environmental variables and habitat suitability using the SDM approach are illustrated by the response curves. The overall shapes of the response curves from both models (Fig. 2) were in general agreement with past studies of spotted owl habitat requirements (e.g., Carey et al., 1990; Hershey et al., 1998; McComb et al., 2002; North et al., 1999; Ripple et al., 1997; Solis & Gutierrez, 1990; Swindle et al., 1999). Habitat suitability decreased quickly with increasing basal area of high elevation forest. Structural characteristics typical of older forests such as greater mean tree height, a higher diversity of tree age classes, and higher vegetative cover were associated with higher habitat suitability estimates. Intermediate

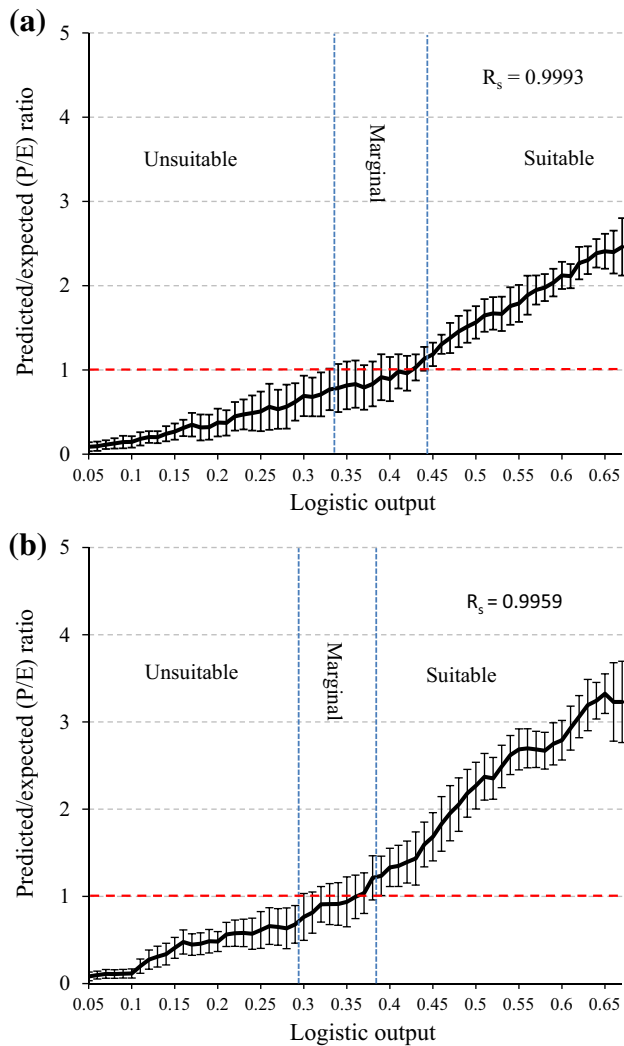


Fig. 3. Predicted/expected ratio curves for Landsat (a) and lidar (b) based models. The predicted/expected ratio is the frequency of occurrences at a particular habitat suitability index predicted by a model divided by the frequency of occurrences expected if the species is randomly distributed.

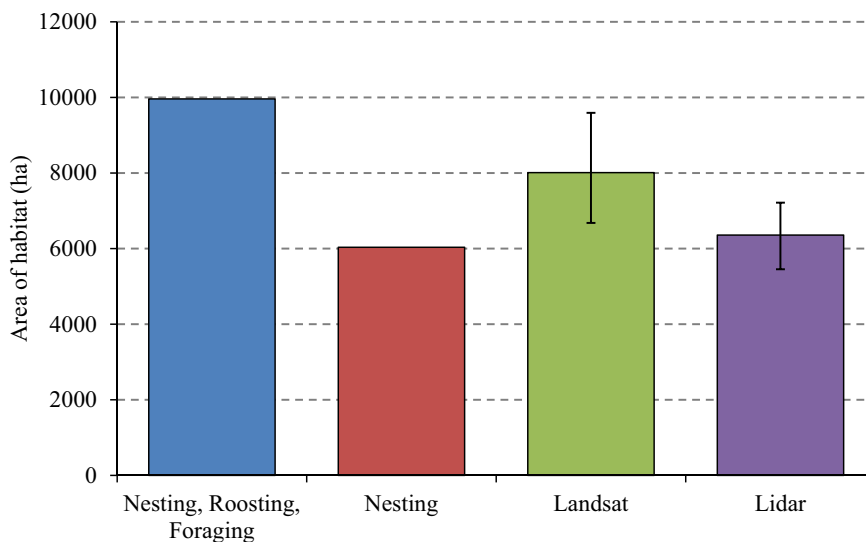


Fig. 4. Habitat area estimates. Error bars are 95% confidence limits for the habitat suitability models (Landsat and lidar). The photo-interpreted map classes (Nesting, Roosting, and Foraging combined and Nesting only) were not empirically derived and do not have error bars.

Table 4

Results of the map comparison analyses. The photo-interpreted maps were considered the user maps for the comparisons with the SDM maps and the lidar map was the user map for the comparison with the Landsat map.

Map statistic	Nesting, roosting, and foraging		Nesting only		Lidar
	vs.		vs.		vs.
	Landsat	Lidar	Landsat	Lidar	Landsat
Omission	0.411	0.440	0.381	0.352	0.281
Commission	0.267	0.123	0.533	0.385	0.429
Kappa	0.380	0.494	0.288	0.495	0.481
Kappa _{loc}	0.475	0.786	0.372	0.517	0.590
Kappa _{histo}	0.800	0.629	0.774	0.957	0.815

densities of large trees were associated with the highest levels of habitat suitability. This may seem counterintuitive, but an important component of spotted owl habitat is large amounts of standing and downed dead trees (e.g., North et al., 1999). This creates gaps in the canopy and hence fewer standing live trees. Also, many of the oldest trees in spotted owl habitat have broken tops which results in an underestimate of the density of large trees when based on height/diameter relationships (Garman et al., 1995). Another factor may have been simply that there were relatively few stands containing grid cells with high values of this variable as reflected by the increased standard deviation above 60 large trees per hectare (Fig. 2).

The predicted/expected ratio curves showed a wider range in the logistic output associated with marginal habitats for the Landsat model than for the lidar model (Fig. 3). This was consistent with the lower model gain estimates for the Landsat model, which indicated less contrast between the presence locations and the background cells. In addition, the lidar produced higher predicted versus expected ratios than the Landsat model, suggesting again higher discrimination between suitable habitat and unsuitable habitat using lidar data.

4.2. Map comparisons

The amount of suitable spotted owl habitat estimated by both SDMs was in good agreement with the habitat map based on aerial photo interpretation (Fig. 4). One advantage that the SDM approach has over photo-interpretation is that it produces maps in an objective framework that can be more easily replicated. There was no predictive accuracy

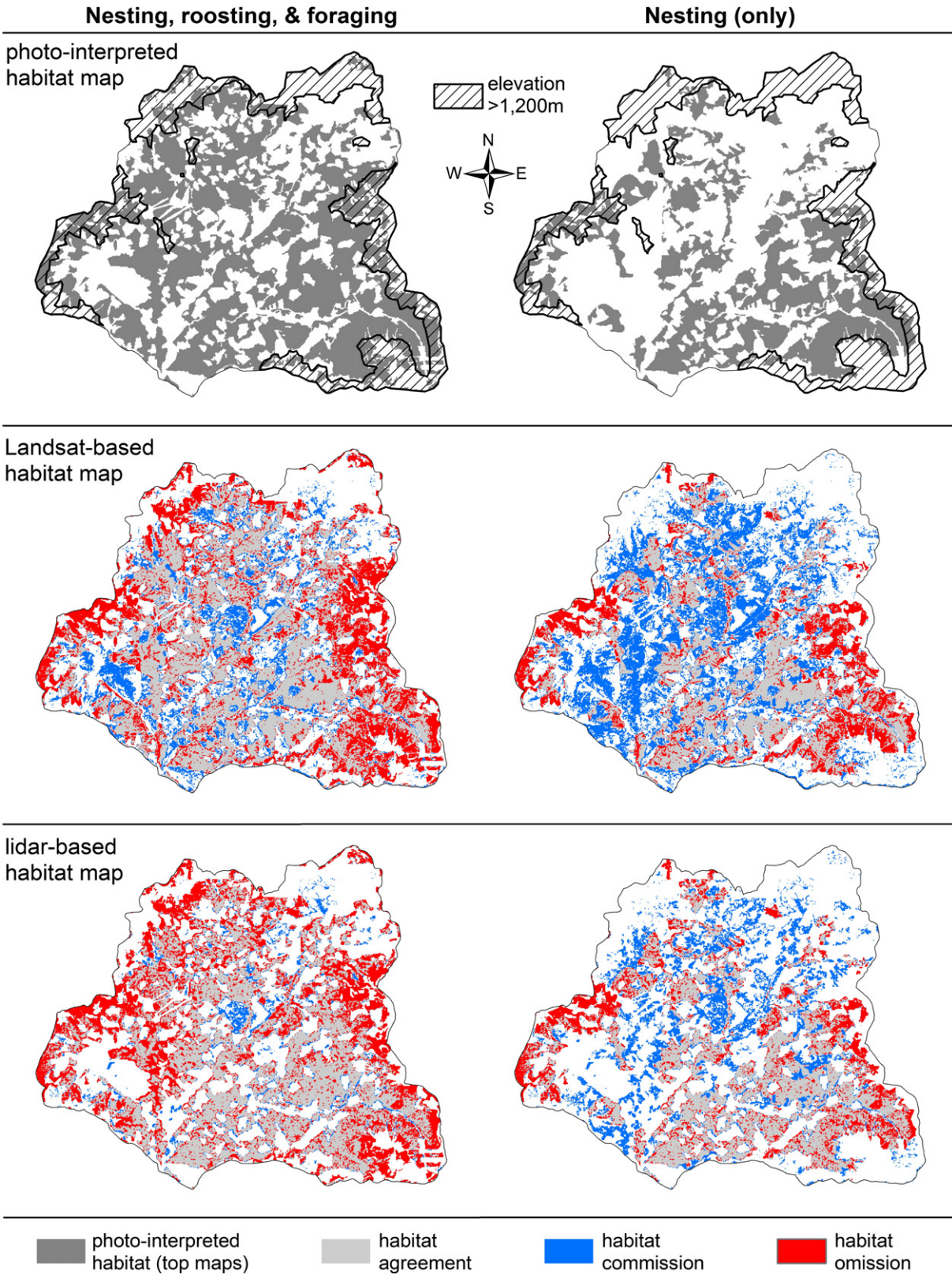


Fig. 5. Spatial patterns of habitat agreement, omission, and commission in the model-based habitat maps relative to the photo-interpreted maps.

assessment available for the photo-interpreted map, as it is based on the field experience of local wildlife biologists. Consequently, it could not be used as a baseline for accuracy assessments of the model based habitat maps. Rather, we used it as a representation of our SDM user's group and compared it to the qualities of each SDM map and whether or not

they provided some degree of confirmation regarding the habitat classifications made by local wildlife biologists.

The Landsat-based habitat model produced estimates of suitable habitat area where the mean was intermediate between the “nesting, roosting, and foraging” and the “nesting only” habitat classes from the

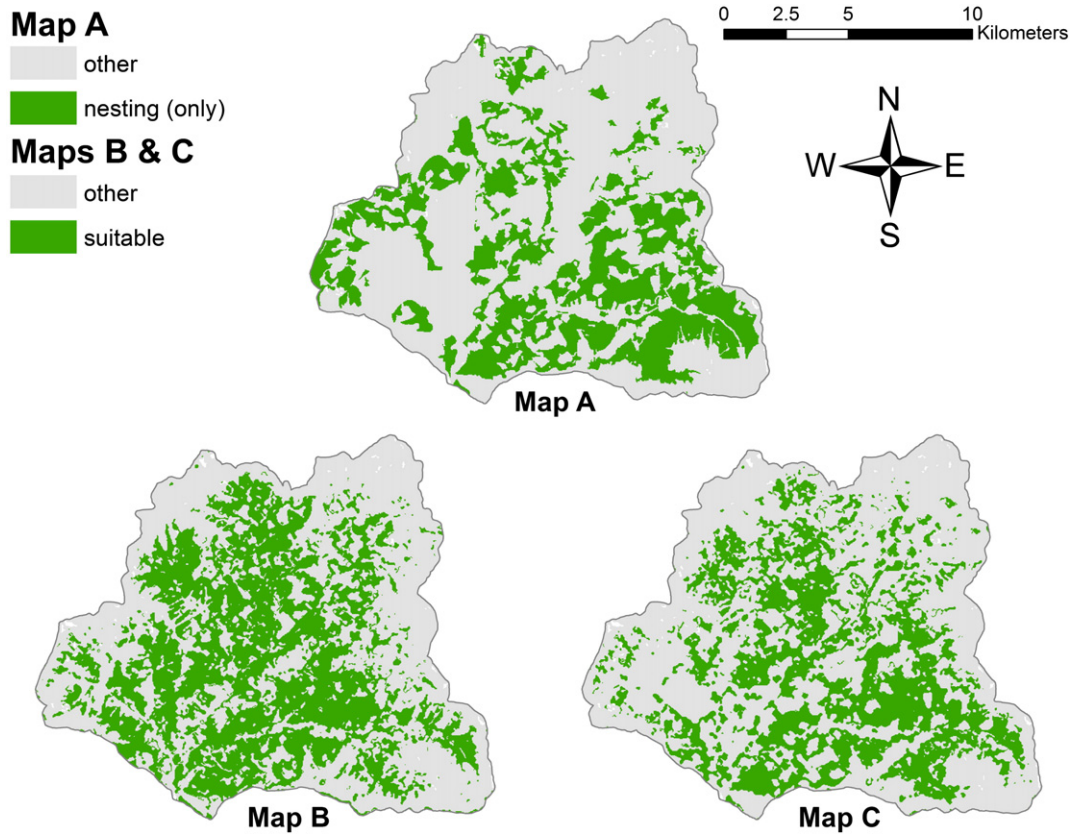


Fig. 6. Reclassified map comparison for the nesting only habitat class from the photo-interpreted map (Map A) and “suitable” habitat from the Landsat (Map B) and lidar (Map C) habitat models.

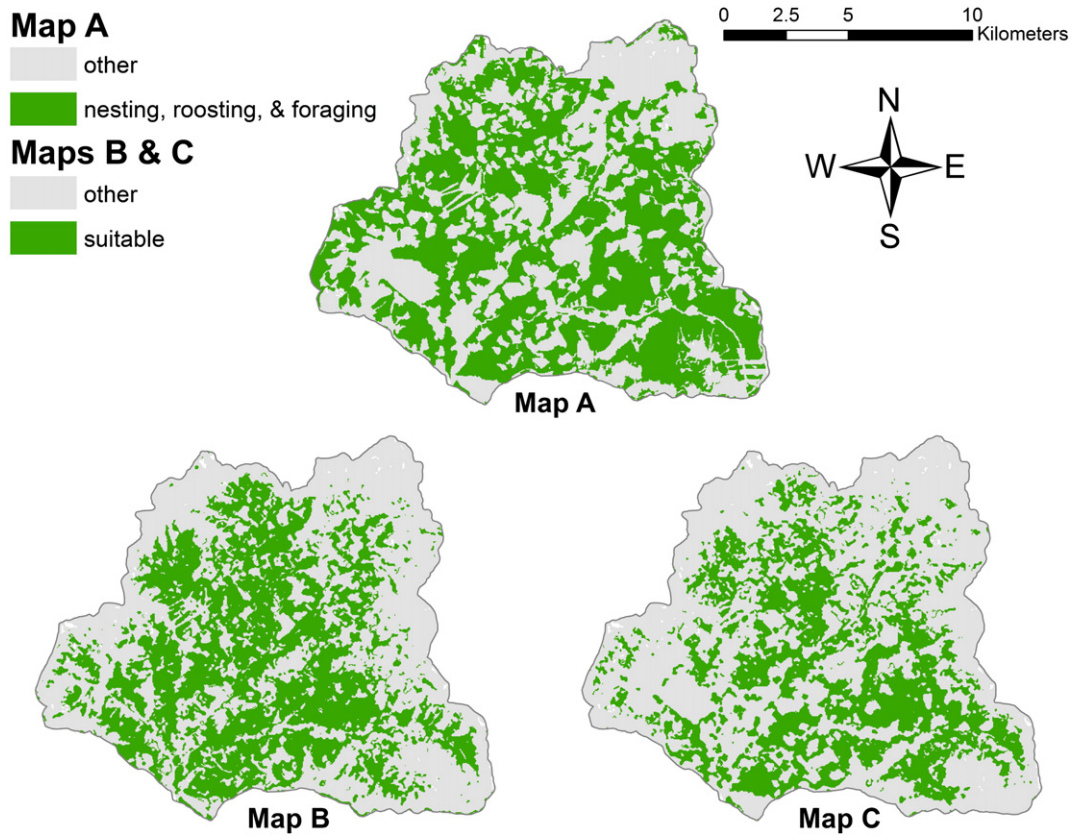


Fig. 7. Reclassified map comparison for the nesting, roosting, and foraging habitat classes from the photo-interpreted map (Map A) and “suitable” habitat from the Landsat (Map B) and lidar (Map C) habitat models.

photo-interpreted map (Fig. 4). The 95% confidence limits for this SDM almost spanned the difference between them. The wider range of habitat quality in the Landsat classification of suitable habitat may include habitat elements necessary for roosting and foraging, but which may not meet the requirements of spotted owls for nesting.

The lidar-based model produced a smaller estimate of suitable habitat area that was very close to what was mapped as “nesting” habitat by local wildlife biologists (Fig. 4). We expect that the reason the lidar-based map was most similar to the “nesting” habitat class from the photo-interpreted map was that the two lidar predictor variables that most influenced model fit and predictive performance, stand height and the density of large trees, were more easily interpreted from aerial imagery than the other predictor variables and are both components of the photo-interpreted definition of nesting habitat. Based on the higher AUC and test gain estimates and the close agreement with the “nesting” habitat class from the photo-interpreted map, we conclude that the lidar-based SDM mapped the spatial arrangement and extent of high quality (i.e., nesting) spotted owl habitat at the watershed scale more reliably than the Landsat-based model.

The photo-interpreted map that combined nesting, roosting, and foraging habitat likely overestimated the amount of spotted owl habitat because photo-interpretation of species composition and an upper elevation limit were not included in the rule-set used to conduct the interpretation (Table 2). As a result, some subalpine forest stands were included in the photo-interpreted versions of habitat which produced high omission rates when compared to the model based maps. Despite the difference in species composition, high elevation forests can have stand structure similar to nesting and roosting habitat when viewed from aerial photos. Spotted owl pairs are rarely found in subalpine forests in this region which suggests that this forest type is not suitable for roosting or nesting. Spotted owls may use subalpine forests for foraging, and the photo-interpreted map included habitat thought to be suitable for foraging. Neither model based map was trained or tested using foraging or dispersal locations, so it is not surprising that subalpine forests were not classified as suitable habitat in the model based habitat maps.

We believe the commission error in the Landsat model was partially due to the inclusion of younger forests with spectral characteristics similar to older forests, perhaps due to aspect or shadows in the canopy. Much of the northwestern half of the study area contains younger forest than the southeastern half, which has more stands that have fully developed into higher quality nesting habitat. Commission also may have been due to complex combinations of environmental covariates that were not easily discernable during aerial photo interpretation. We suspect that the lidar map better distinguished stand structural features associated with nesting that were harder to detect in aerial photographs, or were difficult to map because of the complex pattern they produced in stands that are just transitioning into habitat

4.3. Sampling bias

Measures of predictive performance (i.e., accuracy) estimated by maximum entropy modeling can be affected by biases in the distribution of survey effort (Phillips et al., 2009) and autocorrelation among presence locations (Dormann et al., 2007). By systematically placing survey stations along the road and trail system in the watershed, we obtained a distribution of survey effort throughout the watershed that was not significantly different from a random distribution (Moran's $I = 0.34$, $p = 0.42$). We believe that this distribution of survey effort covered the full range of habitat conditions available to spotted owls in the watershed and did not create a bias in the background samples. We used the nighttime auditory detections obtained from the survey stations only as starting points for daytime searches for nest and roost locations. These detections were typically more dispersed, but much less precise than the roost and nest locations obtained the following day. We felt that the nest and roost locations better reflected habitat selection for features necessary for these important life history

components and that the clumped spatial distribution of the spotted owl nest and roost locations (Moran's $I = 0.66$, $p < 0.01$) was a result of habitat selection and site fidelity and not the result of bias in how the background habitat was sampled.

4.4. Scale considerations

Habitat suitability occurs at a range of scales from the immediate environment surrounding a particular location (e.g., a nest site) to the conditions throughout an animal's home range (e.g., foraging habitat) (e.g., Thompson & McGarigal, 2002). Although using a 30 m grid cell allowed us to delineate and characterize forest stands used by nesting and roosting northern spotted owls, restricting the habitat suitability index to the conditions within individual cells did not reflect the habitat conditions necessary to meet all spotted owl life history requirements. Given that one of our objectives was to compare our lidar-based SDM to a pre-existing habitat suitability map that did not account for habitat selection at different scales, we did not incorporate these considerations here. Future habitat modeling using more extensive lidar coverage would produce more useful habitat suitability models by including landscape level metrics derived from the conditions measured by lidar at fine spatial scales.

Today, scientists, land management and regulatory agency biologists have a multitude of remotely sensed data choices for mapping habitats for species of interest. These data range from coarse spatial resolution multispectral imagery such as Landsat data, to finer spatial resolution imagery such as lidar data. It is sometimes not clear as to which data to use and often the choice depends on the purpose for which the map is being produced. For instance, Landsat data might suffice for broad-scale monitoring of habitat covering millions of hectares over multiple time periods or for identifying large regions that might serve as habitat reserves. Lidar, on the other hand, currently has limited spatial coverage and temporal overlap within the owl's range, thus rendering it impractical for monitoring habitat across the owl's range. However, where it exists, it may be the best choice for mapping habitat within a project area for the purpose of planning and assessing the habitat effects of a management action such as a timber sale.

Lidar data improved upon map precision and predictive performance, producing a map that showed more realistic patterns of habitat that overlaid well with the aerial imagery and the photo-interpreted map produced by wildlife biologists familiar with the area and habitat preferences of northern spotted owls. The Landsat map produced a more general pattern of habitat that did not always fit forest stands visible on aerial photographs at finer resolutions. Lidar data appeared to improve upon the Landsat maps, mainly because it more accurately measured structural attributes of forests that are important to mapping northern spotted owl habitat. However, Landsat combined with environmental and topographic data were still needed to model species composition (Ohmann & Gregory, 2002).

For federally listed threatened species, such as the northern spotted owl, map accuracy is an important consideration for maps that may influence land management decisions and inform species recovery efforts. For example, the Willamette National Forest uses their photo-interpreted map for consultation under Section 7 of the Endangered Species Act. Our results lead us to conclude that the amount of habitat estimated within the confidence limits of Landsat-based models adequately estimated broad scale amounts of habitat, but that lidar-based models produced more precise estimates at finer spatial scales and would be more useful for project level planning.

The cost and effort required to produce vegetation maps designed for a specific purpose also are important considerations for land managers. On the basis of the cost per unit area, lidar becomes increasingly cost effective as the amount of coverage increases (Hummel, Hudak, Uebler, Falkowski, & Megown, 2011). Aerial photo interpretation is typically more expensive and labor intensive than Landsat based approaches, but it also can be more accurate (e.g., Lewis, Phinn, &

Arroyo, 2013). However, creating habitat suitability maps through aerial photo interpretation requires a time consuming and subjective cognitive modeling process which relies on the experience and judgment of human observers and may not be replicable across observers. Once acquired, lidar and Landsat data provide a rich source of input for spatial modeling techniques such as Maxent and GNN, which can provide a faster and more efficient means to objectively create habitat maps.

Acknowledgments

We conducted this research at the H.J. Andrews Experimental Forest, which is funded by the U.S. Forest Service Pacific Northwest Research Station. Spotted owl locations were provided by the central Oregon Cascades northern spotted owl demography study funded by the U.S. Forest Service Pacific Northwest Research Station and Oregon State University (NFS 11-CR-11062756-019). Lidar data was flown and processed by: Watershed Sciences, 257B SW Madison Street Corvallis, OR 97333, www.watershedsciences.com. The lidar data were provided by the H.J. Andrews Experimental Forest research program, funded by the National Science Foundation's Long-Term Ecological Research Program, U.S. Forest Service Pacific Northwest Research Station, and Oregon State University (DEB 08-23380). Dr. Thomas Spies served as principal investigator for the lidar project. Jim Muckenhoupt produced the stem map used for this study. We greatly appreciate the helpful comments provided by Dr. Warren Cohen and an anonymous reviewer on an earlier version of this manuscript. Finally, we wish to acknowledge the hard work and dedication of the many field biologists that provided the nest and roost locations used in this study. Additional financial support was provided by the U.S. Forest Service and the Portland Field Office of the U.S. Fish and Wildlife Service. Any use of trade, firm, or product names is for descriptive purposes only and does not imply endorsement by the U.S. government.

References

- Bergen, K.M., Goetz, S.J., Dubayah, R.O., Henebry, G.M., Hunsaker, C.T., Imhoff, M.L., et al. (2009). Remote sensing of vegetation 3-D structure for biodiversity and habitat: Review and implications for lidar and radar spaceborne missions. *Journal of Geophysical Research*, 114, G00E06. <http://dx.doi.org/10.1029/2008JG000883>.
- Carey, A.B., Reid, J.A., & Horton, S.P. (1990). Spotted owl home range and habitat use in southern Oregon Coast Ranges. *Journal of Wildlife Management*, 54, 11–17.
- Cissel, J.H., Swanson, F.J., & Weisberg, P.J. (1999). Landscape management using historical fire regimes: Blue River, Oregon. *Ecological Applications*, 9, 183–198.
- Cohen, J. (1960). A coefficient of agreement for nominal scales. *Educational and Psychological Measurement*, 20, 37–46.
- Cohen, W.B., Maiersperger, T.K., Spies, T.A., & Oetter, D.R. (2001). Modelling forest cover attributes as continuous variables in a regional context with Thematic Mapper data. *International Journal of Remote Sensing*, 22, 2279–2310.
- Cohen, W.B., & Spies, T.A. (1992). Estimating structural attributes of Douglas fir/western hemlock forest stands from Landsat and SPOT imagery. *Remote Sensing of Environment*, 41, 1–17.
- Cohen, W.B., Spies, T.A., & Bradshaw, G.A. (1990). Semivariograms of digital imagery for analysis of conifer canopy structure. *Remote Sensing of Environment*, 34, 167–178.
- Davis, R.J., Dugger, K.M., Mohoric, S., Evers, L., & Aney, W.C. (2011). Northwest Forest Plan – The first 15 years (1994–2008): Status and trends of northern spotted owl populations and habitats. *General Technical Report PNW-GTR-850*. Portland, OR: U.S. Department of Agriculture, Forest Service, Pacific Northwest Research Station.
- Dixon, G.E., Stage, A.R., Crookston, N.L., Monserud, R.A., Moeur, M., Feguson, D., et al. (2002). Essential FVS: A user's guide to the Forest Vegetation Simulator. *Internal rep.* Fort Collins, CO: U.S. Department of Agriculture, Forest Service, Forest Management Service Center (<http://www.fs.fed.us/fmrc/ftp/fvs/docs/gtr/EssentialFVS.pdf>).
- Dormann, C.F., McPherson, J.M., Araújo, M.B., Bivand, R., Bolliger, J., Carl, G., et al. (2007). Methods to account for spatial autocorrelation in the analysis of species distributional data: A review. *Ecography*, 30, 609–628.
- Dugger, K.M., Anthony, R.G., & Andrews, L.S. (2011). Transient dynamics of invasive competition: Barred owls, spotted owls, habitat, and the demons of competition present. *Ecological Applications*, 21, 2459–2468.
- Elith, J., Phillips, S.J., Hastie, T., Dudik, M., Chee, Y.E., & Yates, C.J. (2011). A statistical explanation of MaxEnt for ecologists. *Diversity and Distributions*, 17, 43–57.
- Eskelson, B.N.I., Temesgen, H., & Barrett, T.M. (2009). Estimating current forest attributes from paneled inventory data using plot-level imputation: A study from the Pacific Northwest. *Forest Science*, 55, 64–71.
- ESRI (Environmental Systems Resource Institute) (2009). *ArcMap 10.0*. Redlands, California, USA: ESRI.
- Fielding, A.H., & Bell, J.F. (1997). A review of methods for the assessment of prediction errors in conservation presence/absence models. *Environmental Conservation*, 24, 38–49.
- Forsman, E.D. (1999). Standardized protocols for gathering data on occupancy and reproduction in spotted owl demographic studies. In J. Lint, B. Noon, R. Anthony, E. Forsman, M. Raphael, M. Collopy, & E. Starkey (Eds.), *Northern spotted owl effectiveness monitoring plan. General Technical Report PNW-GTR-440*. (pp. 32–38). Corvallis, Oregon: U.S. Department of Agriculture, Forest Service, Pacific Northwest Research Station.
- Forsman, E.D., Meslow, E.C., & Wight, H.M. (1984). Distribution and biology of the spotted owl in Oregon. *Wildlife Monographs*, 87, 1–64.
- García-Feced, C., Tempel, D.J., & Kelly, M. (2011). LIDAR as a tool to characterize wildlife habitat: California spotted owl nesting habitat as an example. *Journal of Forestry*, 109, 436–443.
- Garman, S.L., Acker, S.A., Ohmann, J.L., & Spies, T.A. (1995). *Asymptotic height-diameter equations for twenty-four tree species in western Oregon*. Research contribution 10. Corvallis, Oregon: Forest Research Laboratory, Oregon State University.
- Hamer, T.E., Forsman, E.D., & Glenn, E.M. (2007). Home range attributes and habitat selection of barred owls and spotted owls in an area of sympatry. *The Condor*, 109, 750–768.
- Hershey, K.T., Meslow, E.C., & Ramsey, F.L. (1998). Characteristics of forests at spotted owl nest sites in the Pacific Northwest. *Journal of Wildlife Management*, 62, 1398–1410.
- Hirzel, A.H., Le Lay, G., Helfer, V., Randin, C., & Guisan, A. (2006). Evaluating the ability of habitat suitability models to predict species presences. *Ecological Modelling*, 199, 142–152.
- Hummel, S., Hudak, A.T., Uebler, E.H., Falkowski, M.J., & Megown, K.A. (2011). A comparison of accuracy and cost of LiDAR versus stand exam data for landscape management of the Malheur National Forest. *Journal of Forestry*, 109, 267–273.
- Kane, V.R., McGaughey, R.J., Bakker, J.D., Cersonde, R.F., Lutz, J.A., & Franklin, J.F. (2010). Comparisons between field- and LiDAR-based measures of stand structural complexity. *Canadian Journal of Forestry*, 40, 761–773.
- Kelly, E.G., Forsman, E.D., & Anthony, R.G. (2003). Are barred owls displacing spotted owls? *The Condor*, 105, 45–53.
- Lefsky, M.A., Cohen, W.B., Parker, G.G., & Harding, D.J. (2002). Lidar remote sensing for ecosystem studies. *BioScience*, 52, 19–30.
- Lewis, D., Phinn, S., & Arroyo, L. (2013). Cost-effectiveness of seven approaches to map vegetation communities – A case study from northern Australia's tropical savannas. *Remote Sensing*, 5, 377–414.
- Lint, J. B. (tech. coord.) (2005). Northwest Forest Plan – the first 10 years (1994–2003): Status and trends of northern spotted owl populations and habitat. General Technical Report PNW-GTR-648. Portland, OR: U.S. Department of Agriculture, Forest Service, Pacific Northwest Research Station.
- McComb, W.C., McGrath, M.T., Spies, T.A., & Vesely, D. (2002). Models for mapping potential habitat at landscape scales: An example using northern spotted owls. *Forest Science*, 48, 203–216.
- McGaughey, R.J. (2012). *FUSION/LDV: Software for LIDAR data analysis and visualization*. U.S. Department of Agriculture, Forest Service, Pacific Northwest Research Station.
- Mouat, D.A., & Schrumpp, B.J. (1974). Second-year projects and activities of the Environmental Remote Sensing Applications Laboratory (ERSAL). *Annual progress report*. Corvallis, OR: Oregon State University.
- North, M.P., Franklin, J.F., Carey, A.B., Forsman, E.D., & Hamer, T. (1999). Forest stand structure of the northern spotted owl's foraging habitat. *Forest Science*, 45, 520–527.
- Ohmann, J.L., & Gregory, M.J. (2002). Predictive mapping of forest composition and structure with direct gradient analysis and nearest-neighbor imputation in coastal Oregon, USA. *Canadian Journal of Forest Research*, 32, 725–741.
- Ohmann, J.L., Gregory, M.J., Roberts, H.M., Cohen, W.B., Kennedy, R.E., & Yang, Z. (2012). Mapping change of older forest with nearest-neighbor imputation and Landsat time-series. *Forest Ecology and Management*, 272, 13–25.
- Parker, G.G., Harmon, M.E., Lefsky, M.A., Chen, J., Van Pelt, R., Weis, S.B., et al. (2004). Three-dimensional structure of an old-growth *Pseudotsuga-Tsuga* canopy and its implications for radiation balance, microclimate, and gas exchange. *Ecosystems*, 7, 440–453.
- Phillips, S.J., Anderson, R.P., & Schapire, R.E. (2006). Maximum entropy modeling of species geographic distributions. *Ecological Modelling*, 190, 231–259.
- Phillips, S.J., & Dudik, M. (2008). Modeling of species distributions with Maxent: New extensions and a comprehensive evaluation. *Ecography*, 31, 161–175.
- Phillips, S.J., Dudik, M., Elith, J., Graham, C.H., Lehmann, A., Leathwick, J., et al. (2009). Sample selection bias and presence-only distribution models: Implications for background and pseudo-absence data. *Ecological Applications*, 19, 181–197.
- Phillips, S.J., Dudik, M., & Schapire, R.E. (2004). A maximum entropy approach to species distribution modeling. *Proceedings of the Twenty-first International Conference on Machine Learning* (pp. 472–486). New York: ACM Press.
- Ripple, W.J., Lattin, P.D., Hershey, K.T., Wagner, F.F., & Meslow, E.C. (1997). Landscape composition and pattern around northern spotted owl nest sites in southwest Oregon. *Journal of Wildlife Management*, 61, 151–158.
- Solis, D.M., Jr., & Gutiérrez, R.J. (1990). Summer habitat ecology of northern spotted owls in northwestern California. *Condor*, 92, 739–748.
- Swindle, K.A., Ripple, W.J., Meslow, E.C., & Schafer, D. (1999). Old-forest distribution around spotted owl nests in the central Cascade Mountains, Oregon. *Journal of Wildlife Management*, 63, 1212–1221.
- Thompson, C.M., & McGarigal, K. (2002). The influence of research scale on bald eagle habitat selection along the lower Hudson River, New York (USA). *Landscape Ecology*, 17, 569–586.
- U. S. Department of Agriculture, & Forest Service (2007a). Vegetation stand: Willamette National Forest. *GIS geodatabase on file at Willamette National Forest, Supervisors Office, 3106 Pierce Parkway, Suite D, Springfield, Oregon*.

- U. S. Department of Agriculture, & Forest Service (2007b). Definition of spotted owl habitat, Willamette National Forest. *GIS data dictionary/unpublished report on file at Willamette National Forest, Supervisor's Office, 3106 Pierce Parkway, Suite D, Springfield, Oregon.*
- U. S. Department of Agriculture, Forest Service, & U. S. Department of the Interior, Bureau of Land Management (1994). *Record of decision for amendments to Forest Service and Bureau of Land Management planning documents within the range of the northern spotted owl. Standards and guidelines for management of habitat for late-successional and old-growth forest related species within the range of the northern spotted owl.* (Washington, D. C., Sections numbered separately).
- U. S. Department of the Interior, Fish and Wildlife Service (1990). Endangered and threatened wildlife and plants: Determination of threatened status for the northern spotted owl. *U. S. Federal Register*, 55, 26114–26194.
- Visser, H., & de Nijs, T. (2006). The map comparison kit. *Environmental Modeling and Software*, 21, 346–358.
- Wiens, J.D., Anthony, R.G., & Forsman, E.D. (2011). Barred owl occupancy surveys within the range of the northern spotted owl. *Journal of Wildlife Management*, 75, 531–538.